

---

# Bayesian Telephone: Memory Consolidation and Recall as Generative Processes

---

Dongyu Gong

Yale University

dongyu.gong@yale.edu

Micah Gold

Yale University

micah.gold@yale.edu

## Abstract

1 The hippocampus serves a key role in memory acquisition and consolidation, yet it  
2 is unknown whether the hippocampus stores raw sensory inputs or merely generative  
3 reconstructions of those inputs. In this paper we examined these competing  
4 hypotheses of memory representation in the hippocampus. To do so we modeled  
5 the hippocampus as a modern Hopfield network and the entorhinal cortex as a variational  
6 autoencoder (VAE). We used Mitsuba 3 to generate a Cornell box dataset.  
7 In our first model, we passed these scenes directly into our Hopfield network and  
8 trained our VAE on the Hopfield network's output when prompted by stimulus.  
9 In the second, the model first probabilistically inferred latent parameters for the  
10 observations and generated reconstructed observations which were then passed into  
11 the Hopfield network to aid in the training of our VAE. We tested the capacity of  
12 our models for generative recall of these scenes and found reliable minimization  
13 of reconstruction error during recall in both models. We concluded that either  
14 representation scheme or a combination of the two might be at work in the human  
15 brain. Future studies should explore implementing features such as forgetting and  
16 recall vulnerability in our base model and comparing model performance to human  
17 performance on recall tasks.

18 

## 1 Introduction

19 Memory is at the core of human cognition. Understanding the algorithms of how we encode, store,  
20 retrieve, and use memory representations is essential for understanding human intelligence.

21 Simply put, human memory is characterized by the lossy compression and imperfect reconstruction of  
22 an initial set of neural signals associated with sensory experiences. In order to construct and maintain  
23 a memory, the mind must first learn "schemas" (latent structures) from sensory inputs [10]. The  
24 hippocampus is responsible for directing the initial parsing of stimuli into memories. Over time, the  
25 hippocampus mediates the transfer of relevant patterns of neural activity through the entorhinal cortex  
26 (EC) to the medial prefrontal cortex and anterolateral temporal cortex via "neural replay" [4, 21, 22].  
27 This process of consolidation entails the learning of schemas and enables the creation of longer-  
28 term memory. Long-term memories can persist in the neocortex for a lifetime, but the process of  
29 "accessing" these memories is anything but straightforward [3]. Recall entails utilizing these learned  
30 schemas stored in the neocortex to realize a noisy estimation of aspects of the initial brain state at the  
31 time of first memory acquisition [18].

32 This whole process can be framed as the training of a generative model and the subsequent generative  
33 processes mediated by the latent variables learned by the model. However, a complete understanding  
34 of the inner-workings of the memory formation process remains remote [9, 15]. For one, it is unclear  
35 just exactly how short-term memories are represented in the hippocampus and when along the  
36 complex process of memory consolidation the initial armada of neural signals are stripped down to  
37 that more fine set responsible for encoding latents. Perhaps there are even multiple layers of Bayesian  
38 inference and image regeneration inherent in the pathways of memory formation.

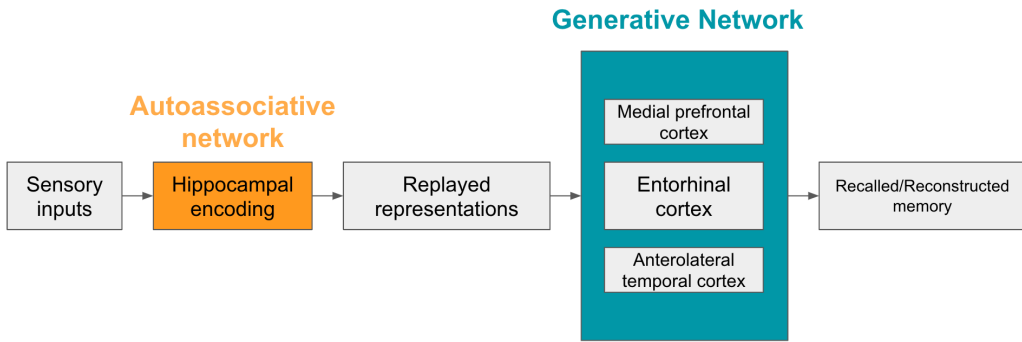


Figure 1: Model of the consolidation-recall pathway that allows for long-term memory formation. The hippocampus acts as an autoassociative network which stores encodings of sensory inputs. Over time, replay of these representations facilitates the learning of latent structures by the neocortex. The neocortex then acts as a generative network, producing noisy recollections of memories from these learned parameters on demand.

39 To grapple with these questions, recent studies have reverse engineered computationally plausible  
40 models of the consolidation-recall pathway. Many of these studies model the hippocampus as an  
41 autoassociative network and the neocortex as a generative network [17]. One such study of interest,  
42 devised a system by which a modern Hopfield network, representing the hippocampus, employed  
43 teacher-student learning [11] to train a variational autoencoder (VAE) representing the EC [19].  
44 This model proved capable of robust generative recall when the Hopfield network encoded exact  
45 representations of images.

46 Here, we examine whether and how altering the encoding mechanism in the Hopfield network might  
47 impact the capacity of the model for generative recall. Specifically we compare the performance of an  
48 exact reimplementation of the original model with one in which the Hopfield network instead stores  
49 reconstructions of the scenes after an initial layer of Bayesian inference and image regeneration. In  
50 doing so, we attempt to understand whether the hippocampus aids the neocortex in learning latent  
51 structures from raw sensory inputs or stochastic reconstructions of sensory inputs (i.e. perception). In  
52 other words, we seek to shed light on whether consolidation is merely the learning of latents from  
53 observations or rather the learning of latents from reconstructed observations which themselves result  
54 from a long game of Bayesian telephone.

## 55 2 Methods

56 Code for the methods described below can be accessed in this repository: <https://github.com/>  
57 Daniel-Gong/final\_project.

### 58 2.1 Custom Cornell Box Dataset

59 Using Mitsuba 3 we constructed a dataset (see Figure 3) of 270 Cornell box images each  
60 with a distinct combination of wall color (`{red, white, green}`), floor color (`{red, white,`  
61 `green}`), feature shape (`{sphere, cube}`), feature color (`{red, white, green}`), and feature  
62 scale (`{.3, .4, .5, .6, .7}`).

### 63 2.2 Inverse Graphics Engine

64 Using the Gen package for Julia [6], we implemented an inverse graphic engine capable of inferring  
65 latent parameters from each observation in our dataset and reconstructing noisy images from these  
66 latents. Inference was conducted by constraining the generative function with bitmaps of the original  
67 observations selectively compressed to ensure representative description of the key-features of the

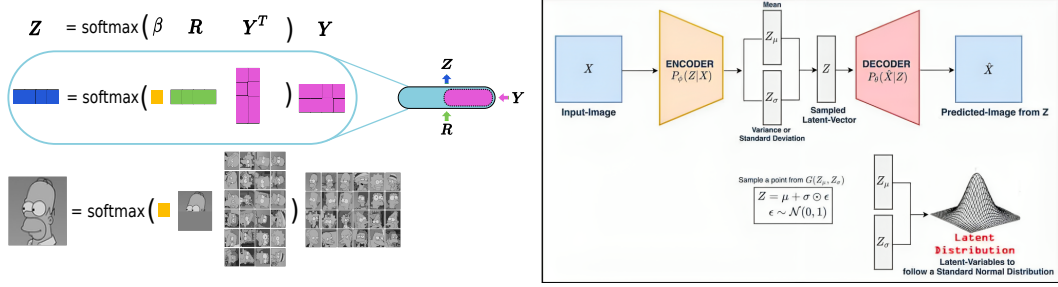


Figure 2: Model illustrations. **Left:** pattern retrieval process in the modern Hopfield network.  $Z$  is the pattern to be retrieved,  $Y$  are all stored patterns,  $R$  is the input pattern, and  $\beta$  is the inverse temperature parameter. **Right:** architecture of the variational autoencoder. The process begins with the input image fed into the encoder, which encodes the image into a latent representation characterized by a mean vector and a variance or standard deviation vector. From this, a sampled latent vector is generated, where the latent variable  $Z$  is sampled as  $Z = \mu + \sigma \odot \epsilon$ , with  $\epsilon$  drawn from a standard normal distribution  $\mathcal{N}(0, 1)$ . The decoder then takes the sampled latent vector to reconstruct the predicted image from  $Z$ , which is the VAE’s approximation of the original image.

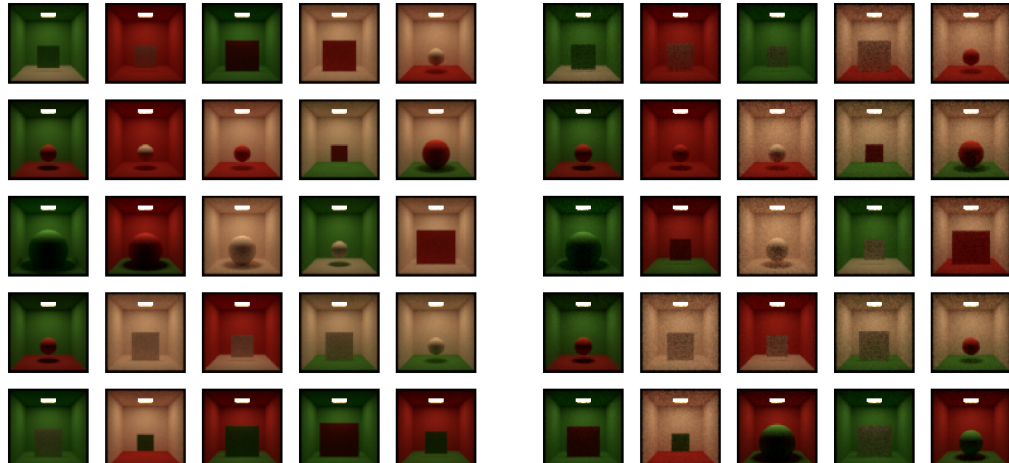


Figure 3: **Left:** 25 examples from our custom Cornell box dataset. **Right:** 25 inferred Cornell box images, corresponding to the ones on the left.

68 observations. Using Bayes rule a posterior for the latents was generated over these bitmaps:

$$P(\theta|b(I)) \propto P(b(I)|\theta)P(\theta) \quad (1)$$

69 where  $\theta$  are latents, and  $b(I)$  are bitmap observations. Random-walk Metropolis-Hastings algorithm  
70 was employed to sample latent values for each image from their respective posteriors.

### 71 2.3 Modern Hopfield Network

72 We implemented a modern Hopfield network to model the hippocampus using the TensorFlow  
73 package for Python (accessed via PyCall in Julia) [1]. Modern Hopfield networks are a variety of  
74 recursive neural network designed to model dense associative memory. In a modern Hopfield network,  
75 stable state corresponds to a particular memories [16, 13]. Compared to their classical alternatives,  
76 modern Hopfield networks are better suited for modeling biological memory because they maintain  
77 exponential storage capacity per neuron and differentiability across use cases [13]. A core equation  
78 for the modern Hopfield network we are using (see Figure 2 left panel) is the update rule for the  
79 state of the stored patterns, which is based on the concept of continuous states and uses an attention  
80 mechanism [16]. This can be represented as:

$$\mathbf{Z} = \text{softmax}(\beta \mathbf{R} \mathbf{Y}^T) \mathbf{Y} \quad (2)$$

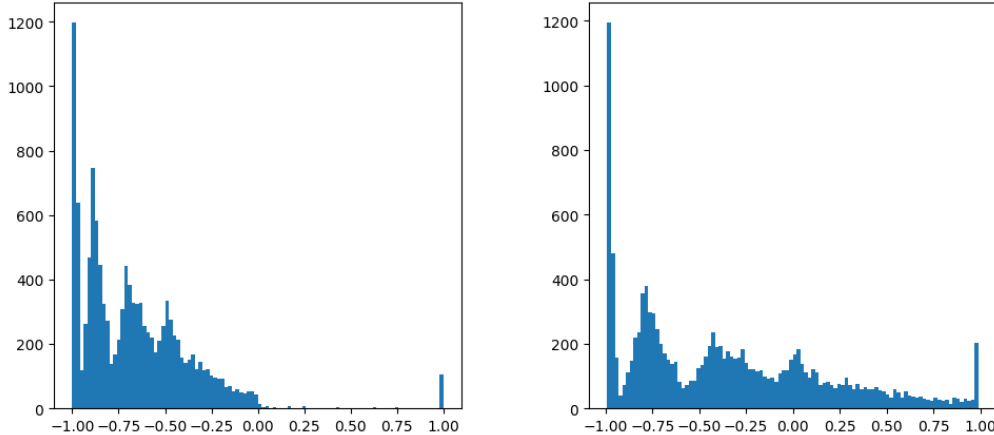


Figure 4: **Left:** Histogram of pixel values of one example image from our custom Cornell box dataset before normalization. **Right:** histogram of pixel values of the same image after normalization.

81 where  $\mathbf{Z}$  is the state vector of the Hopfield network,  $\mathbf{Y}$  is the matrix of stored patterns (weights),  $\mathbf{R}$  is  
 82 the input pattern,  $\beta$  is the inverse temperature parameter, controlling the sharpness of the softmax  
 83 function. The softmax function is applied to ensure that the output is a probability distribution. This  
 84 formula demonstrates how the attention mechanism is used in modern Hopfield networks, in which  
 85 the similarity between the input pattern and the stored patterns determines the weights used to update  
 86 the network's state.

87 We used uniform random noise inputs (between -1 and 1) as the input pattern to initiate pattern  
 88 retrieval ("neural replay") from the Hopfield network. To make sure all stored patterns (no matter  
 89 they are spheres or cubes) have equal probabilities to be replayed, we normalized the distribution of  
 90 pixel values in the stored patterns to be between -1 and 1 (see Figure 4).

#### 91 2.4 Variational Autoencoder

92 We implemented a VAE to model the EC using the TensorFlow package for Python (accesed via PyCall  
 93 in Julia) [1]. Variational autoencoders are generative networks that learn to deconstruct observations  
 94 into latent parameters from which those initial observations can be nosily reconstructed [12]. Our  
 95 VAE (see Figure 2 right panel) was trained to minimize the reconstructed error between input images  
 96 (i.e., replayed memories from the modern Hopfield network) and predicted images from the decoder,  
 97 as well as the Kullback-Leibler (KL) divergence between the latent vector sampled in VAE and a  
 98 standard normal distribution. The loss function of our VAE can be represented as:

$$L(\phi, \theta, x) = \frac{1}{N} \sum_{i=1}^N (X_i - \hat{X}_i)^2 + KL(G(Z_\mu, Z_\sigma) || \mathcal{N}(0, 1)) \quad (3)$$

99 where  $\phi$  are the parameters of the encoder,  $\theta$  are the parameters of the decoder,  $X_i$  is the  $i$ th input  
 100 image replayed from the Hopfield network,  $\hat{X}_i$  is the  $i$ th reconstructed image produced by the  
 101 decoder, and  $N$  is the total number of images in the dataset ( $N = 270$  in our case).  $G(Z_\mu, Z_\sigma)$  is  
 102 the Gaussian distribution defined by the encoder's output, which includes a mean vector  $Z_\mu$  and a  
 103 standard deviation vector  $Z_\sigma$ . The first term on the right side of this equation is a Mean-Squared-Error  
 104 (MSE) loss, and the second term (the KL divergence) acts as a regularizer, which keeps the encodings  
 105 sufficiently diverse.

106 We used the AMSGrad variant of the Adam optimiser as the stochastic gradient descent method for  
 107 the training of the VAE. A latent variable vector length of 20, learning rate of 0.001 and KL weighting  
 108 of 1 were used in the main results.

109 To test the performance of our VAE after training, we created perturbed partial Cornell box images  
 110 by randomly selecting 10% of pixels in each image and then replacing them with 0s. These partial  
 111 images are used as the input to the trained VAE to check their generative recall.

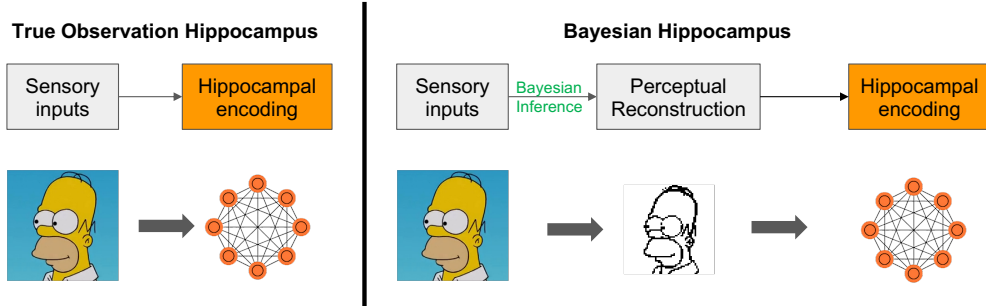


Figure 5: Two hypotheses. **Left:** The memory storage mechanism for the true observation hippocampus hypothesis simply entails storing the original sensory inputs to the Hopfield network. **Right:** The memory storage mechanism for the Bayesian hippocampus hypothesis entails passing the sensory inputs into the inverse graphics engine and capturing the perceptual reconstruction in the Hopfield network.

## 112 2.5 Two Hypotheses

### 113 2.5.1 True Observation Hippocampus

114 In this hypothesis (Figure 5 left panel), sensory inputs are stored in the hippocampus exactly as they  
 115 are observed. In order to model this, the original 270 images from our Cornell Box dataset were  
 116 stored in the modern Hopfield network. Next, we exposed the Hopfield network to random noises and  
 117 recorded which observations were replayed. We passed in the replayed representations and trained the  
 118 VAE over 50 epochs (with early stopping applied if there was no loss improvement for three epochs)  
 119 to learn the encoding of those stimuli as latents which could then be decoded to generatively "recall"  
 120 observations similar to those original observations stored in the Hopfield network. The reconstruction  
 121 error of the VAE with respect to the replayed representations from the Hopfield network was analyzed  
 122 to shed light on the utility of the model.

### 123 2.5.2 Bayesian Hippocampus

124 In this hypothesis (Figure 5 right panel), sensory inputs are first passed into our inverse graphics  
 125 engine for preprocessing. The inverse graphics engine infers latent parameters from those images  
 126 and constructs noisy perceptions of the images. These reconstructions are passed into the modern  
 127 Hopfield network and stored as memories. We exposed the Hopfield network to random noises and  
 128 recorded replayed observations. As before, we passed in the replayed representations and trained the  
 129 VAE over 50 epochs (with early stopping applied if there was no loss improvement for three epochs)  
 130 to learn the latents underlying these representations so as to reconstruct them. The reconstruction  
 131 error of the VAE was analyzed to shed light on the appropriateness of the Bayesian hippocampus  
 132 hypothesis as compared with the true observation hippocampus hypothesis.

## 133 3 Results

### 134 3.1 True Observation Hypothesis

135 After 270 images from our custom Cornell box dataset were encoded in the modern Hopfield network,  
 136 random noise inputs to the network successfully reactivated its memories (Figure 6). Notably, our  
 137 normalization procedure on the distribution of pixel values ensured that all stored patterns had a  
 138 chance to be replayed, no matter what shape they are, what color they have, etc. It is possible that  
 139 this normalization procedure is also implemented in the brain to ensure better encoding and retrieval  
 140 of memories [8, 5], considering that the neural signals of sensory experiences can vary a lot in terms  
 141 of their salience merely because of their physical properties.

142 The training of our VAE on the replayed true observations converged after around 15 epochs and  
 143 triggered early stopping after around 30 epochs. The performance test for the trained VAE showed

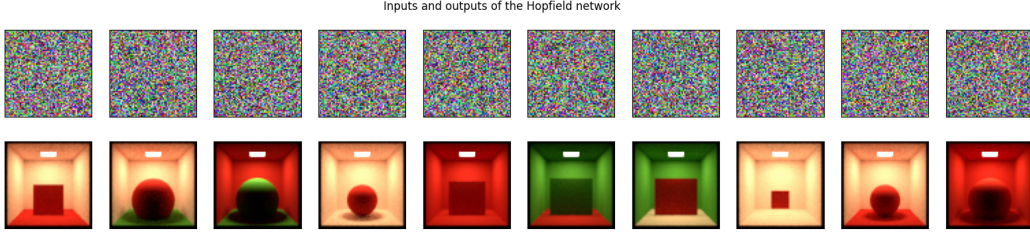


Figure 6: True observation hypothesis: random inputs to the Hopfield network and the corresponding replayed true observations.

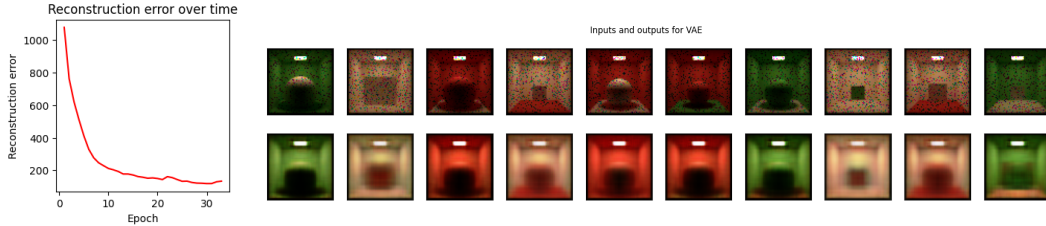


Figure 7: True observation hypothesis. **Left:** reconstruction errors of the VAE across training epochs. **Right:** VAE reconstructions based on noisy Cornell box images.

144 that it was able to noisily reconstruct complete observations from perturbed partial images in the  
 145 original custom Cornell box dataset (Figure 7). The recalled memories are to some degree sketchy  
 146 and blurry given that there are only 270 training images. However, we believe scaling up the number  
 147 training samples will lead to significantly better performance.

### 148 3.2 Bayesian Hypothesis

149 First, our inverse inverse graphics engine for the most part generated images that differed only slightly  
 150 from the original images (Figure 3 right panel), even though we only used a simple random walk  
 151 Metropolis Hastings algorithm. As before, we applied the same normalization procedure to make  
 152 sure every inferred image has a chance to be replayed after they are encoded in the Hopfield network.  
 153 Random noise inputs to the network successfully reactivated diverse memories (Figure 8).

154 Furthermore, the training of our VAE on the replayed inferred images converged also after around  
 155 15 epochs and triggered early stopping after around 40 epochs. The performance test for the trained  
 156 VAE showed that it was also able to noisily reconstruct complete observations from perturbed partial  
 157 images in the original custom Cornell box dataset (Figure 9).

## 158 4 Discussion

159 Although the quality of our reconstructed images is somewhat impressive, we must first acknowledge  
 160 a few constraints on our experiment that reduced the performance of both models and influenced our  
 161 results. Firstly, given issues with accessing large compute resources on short notice we opted to train  
 162 our models on smaller dataset of 270 images whereas other similar studies using VAE's recommend  
 163 upwards of 10,000 images [12, 19]. Secondly, we built our inverse graphics engine in our Bayesian  
 164 hypothesis to infer a measly six parameters, five of which were drawn from discrete distributions.  
 165 As a result, the reconstructed images were in some ways too similar to our original images and in  
 166 some ways unrealistically different. For example, in our model either the exact hue of red, white, or  
 167 green was inferred or the incorrect color was inferred altogether. In reality however it is much more  
 168 plausible that a human would infer a lightish-red ball to be a darkish-pink ball than a white ball.

169 Still, despite these issues both the true observation and Bayesian hypotheses demonstrated equal  
 170 proficiency in recalling memories from noisy inputs. Considering that the brain's inverse graphic  
 171 engine likely possesses comparable or greater strength than our implemented graphics engine for  
 172 this task, this suggests that the hippocampus could represent memories in either fashion while  
 173 yielding similar success in recall. Unfortunately, this leads to the conclusion that both models would

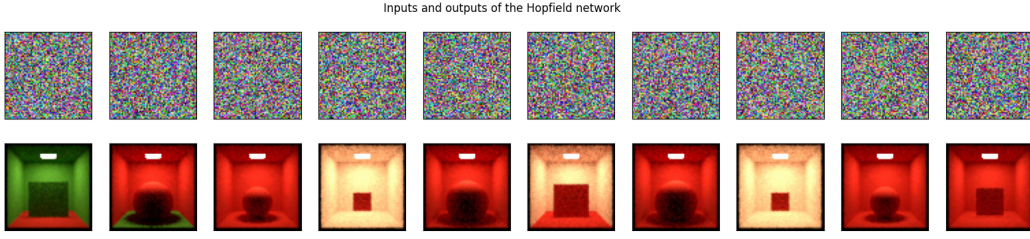


Figure 8: Bayesian hypothesis: random inputs to the Hopfield network and the corresponding replayed Bayesian inferences.



Figure 9: Bayesian hypothesis. **Left:** reconstruction errors of the VAE across training epochs. **Right:** VAE reconstructions based on noisy Cornell box images.

174 perform similarly if we compared their recall performance against human subjects. Thus, employing  
 175 behavioral comparison metrics between our model and human subject would be insufficient to fully  
 176 pick open the neural black-box and understand the fine mechanisms of the hippocampus.

177 On the flip side, the success of both hypotheses highlights an intriguing principle regarding how  
 178 and when the brain may opt to deal with true observations as opposed to reconstructed observations.  
 179 Since the computational outcome remains consistent, the brain might decide whether to utilize  
 180 Bayesian reconstructions or original observations based on minimizing the temporal and spatial  
 181 complexity of the system. In other words, algorithmically speaking, the brain might choose the  
 182 representation that is more practically convenient. If this holds true, then considering our two models  
 183 of hippocampal memory representation as mutually exclusive would be inaccurate. It is plausible that  
 184 the hippocampus could store images, reconstructions of images from inferred latents, and perhaps  
 185 even the latents themselves [19]. To test this hypothesis, future work should attempt to integrate all  
 186 three forms of memory representation into the same Hopfield network. Surmising which hippocampal  
 187 representation is in use any given moment in consolidation could be a matter of recording neural  
 188 population dynamics during memory acquisition tasks in humans and comparing these dynamics to  
 189 simulated traces from this integrated model [14].

190 Collecting behavioral data on similar recall tasks could also be useful to help direct the refinement of  
 191 our overall model of generative recall and build in even more complex functionalities. For example,  
 192 the current model only implicitly handles the possibility of forgetting images. True, consolidating  
 193 additional memories in our model reduces the probability of recalling a prior memory. However,  
 194 this is only because given a stimuli our model recalls a memory and the more similar memories  
 195 there are stored in the VAE, the smaller the chance of a particular memory being recalled. A more  
 196 robust system of forgetting, must consider the larger biological picture of the issue: there is a limited  
 197 quantity of data that can physiologically be stored in both the hippocampus and the neocortex and a  
 198 limited amount of time memories are stored in the hippocampus during which they can be replayed  
 199 and consolidated and transferred to the neocortex. As a result, forgetting could be the result of either  
 200 temporal constraints (the hippocampus selectively participating in the consolidation of one decaying  
 201 memory at the expense of another) or spatial constraints (rewiring neural pathways in the neocortex  
 202 resulting in the loss of particular activation dynamics) [7, 20]. Accessing behavioral data on the rate  
 203 and nature of "forgetting" and the influence of recall on reconsolidating images (and thus increasing  
 204 their likelihood of being recalled on future occasions) could guide the creation of a more robust  
 205 probabilistic forgetting system.

206 In a similar vein, the current model does not implement any sort of system emulating recall vulnera-  
 207 bility [2], the phenomenon by which generatively recalling memory results in increased malleability  
 208 of the associated learned latent structures in the neocortex. Although we experimented with an

209 implementation of a probabilistic system capable of occasionally adding the products of generative  
210 recall to the Hopfield network and retraining the VAE with these noisy "hallucinated" memories, we  
211 faced difficulties in determining how to (1) tune the parameters of such a system to accurately reflect  
212 the realities of recall vulnerability (which has not been extensively quantitatively studied) and (2)  
213 rebuild our memory acquisition model in a sequential manner to avoid having to retrain the entire  
214 VAE every time recall affected our Hopfield network.

215 Hence, our base model represents a strong jumping-off point for future exploration of the generative  
216 processes that underlie episodic and semantic memory, imagination and recall. Refining our model  
217 piece-by-piece to bring it in line with behavioral results could yield key insights into the neural fabric  
218 of memory and the computational and algorithmic systems that govern our lives.

## 219 References

- 220 [1] Martín Abadi, Paul Barham, Jianmin Chen, and et al. Tensorflow: A system for large-scale  
221 machine learning. 2016. [arXiv:1605.08695](https://arxiv.org/abs/1605.08695).
- 222 [2] Cristina M Alberini. The role of reconsolidation and the dynamic process of long-term memory  
223 formation and storage. *Frontiers in Behavioral Neuroscience*, 5:12, 2011. doi:10.3389/  
224 fnbeh.2011.00012.
- 225 [3] Craig H. Bailey, Eric R. Kandel, and Kausik Si. The persistence of long-term memory: A  
226 molecular approach to self-sustaining changes in learning-induced synaptic growth. *Neuron*,  
227 44:49–57, 2004. doi:10.1016/j.neuron.2004.09.017.
- 228 [4] Michael F Bonner and Alfonso R Price. Where is the anterior temporal lobe and what does  
229 it do? *The Journal of neuroscience : the official journal of the Society for Neuroscience*,  
230 33(10):4213–4215, 2013. doi:10.1523/JNEUROSCI.0041-13.2013.
- 231 [5] Matteo Carandini and David J. Heeger. Normalization as a canonical neural computation.  
232 *Nature Reviews Neuroscience*, 13(1):51–62, January 2012. doi:10.1038/nrn3136.
- 233 [6] Marco Cusumano-Towner, Feras Saad, Alexander Lew, and Vikash Mansinghka. Gen: A  
234 general-purpose probabilistic programming system with programmable inference. 11 2018.
- 235 [7] Ronald L Davis and Yi Zhong. The biology of forgetting-a perspective. *Neuron*, 95(3):490–503,  
236 2017. doi:10.1016/j.neuron.2017.05.039.
- 237 [8] Narges Doostani, Gholam-Ali Hosseini-Zadeh, and Maryam Vaziri-Pashkam. The normalization  
238 model predicts responses in the human visual cortex during object-based attention. *eLife*,  
239 12:e75726, April 2023. doi:10.7554/eLife.75726.
- 240 [9] Tom Hartley, Chris M. Bird, Dennis Chan, Lisa Cipolotti, Masud Husain, Faraneh Vargha-  
241 Khadem, and Neil Burgess. The hippocampus is required for short-term topographical memory  
242 in humans. *Hippocampus*, 17(1):34–48, 2007. doi:10.1002/hipo.20240.
- 243 [10] P. Hemmer and M. Steyvers. A bayesian account of reconstructive memory. *Topics in Cognitive  
244 Science*, 1(1):189–202, 2009.
- 245 [11] Geoffrey Hinton, Oriol Vinyals, Jeff Dean, and et al. Distilling the knowledge in a neural  
246 network. *arXiv preprint arXiv:1503.02531*, 2(7), 2015.
- 247 [12] Diederik P Kingma and Max Welling. Auto-encoding variational bayes. 2022. [arXiv:  
248 1312.6114](https://arxiv.org/abs/1312.6114).
- 249 [13] Dmitry Krotov and John J Hopfield. Dense associative memory for pattern recognition, 2016.  
250 [arXiv:1606.01164](https://arxiv.org/abs/1606.01164).
- 251 [14] Hsin-Hung Li and Clayton E. Curtis. Neural population dynamics of human working memory.  
252 *Current Biology*, 33(17):3775–3784.e4, 2023. URL: [https://www.sciencedirect.com/  
253 science/article/pii/S0960982223010394](https://www.sciencedirect.com/science/article/pii/S0960982223010394), doi:10.1016/j.cub.2023.07.067.
- 254 [15] Alison R. Preston and Howard Eichenbaum. Interplay of hippocampus and prefrontal cortex in  
255 memory. *Current Biology*, 23(17):R764–R773, 2013. doi:10.1016/j.cub.2013.05.041.

- 256 [16] Hubert Ramsauer, Bernhard Schäfl, Johannes Lehner, Philipp Seidl, Michael Widrich, Thomas  
257 Adler, Lukas Gruber, Markus Holzleitner, Milena Pavlović, Geir Kjetil Sandve, Victor Greiff,  
258 David Kreil, Michael Kopp, Günter Klambauer, Johannes Brandstetter, and Sepp Hochreiter.  
259 Hopfield networks is all you need. 2021. arXiv:2008.02217.
- 260 [17] Edmund T Rolls. A quantitative theory of the functions of the hippocampal ca3 network in  
261 memory. *Frontiers in cellular neuroscience*, 7:98, 2013. doi:10.3389/fncel.2013.00098.
- 262 [18] D. L. Schacter. Adaptive constructive processes and the future of memory. *American Psycholo-*  
263 *gist*, 67(8):603–613, 2012. doi:10.1037/a0029869.
- 264 [19] Eleanor Spens and Neil Burgess. A generative model of memory construction and consolidation.  
265 *bioRxiv*, page 2023.01.19.524711, 01 2023. doi:10.1101/2023.01.19.524711.
- 266 [20] Larry R Squire, Lisa Genzel, John T Wixted, and Richard G Morris. Memory consolida-  
267 tion. *Cold Spring Harbor perspectives in biology*, 7(8):a021766, 2015. doi:10.1101/  
268 cshperspect.a021766.
- 269 [21] Joel L. Voss, Donna J. Bridge, Neal J. Cohen, and Jeffrey A. Walker. A closer look at  
270 the hippocampus and memory. *Trends in Cognitive Sciences*, 21(8):577–588, 2017. doi:  
271 10.1016/j.tics.2017.05.008.
- 272 [22] H Freyja Ólafsdóttir, Daniel Bush, and Caswell Barry. The role of hippocampal replay in  
273 memory and planning. *Current Biology*, 28(1):R37–R50, 2018. doi:10.1016/j.cub.2017.  
274 10.073.